Macromolecular Research, Vol. 14, No. 1, pp 59-65 (2006)

Effect of Collector Temperature on the Porous Structure of Electrospun Fibers

Chi Hun Kim, Yoon Ho Jung, Hak Yong Kim*, and Douk Rae Lee

Department of Textile Engineering, Chonbuk National University, Chonju 561-756, Korea

Nallasamy Dharmaraj

Department of Chemistry, Government Arts College, Udumalpet – 642 126, India

Kyung Eun Choi

Department of Practical Art Education, Chonju National University of Education, Chonju 560-757, Korea

Received October 6, 2005; Revised November 21, 2005

Abstract: We report a new approach to fabricate electrospun polymer nonwoven mats with porous surface morphology by varying the collector temperature during electrospinning. Polymers such as poly(L-lactide) (PLLA), polystyrene (PS), and poly(vinyl acetate) (PVAc) were dissolved in volatile solvents, namely methylene chloride (MC) and tetrahydrofuran (THF), and subjected to electrospinning. The temperature of the collector in the electrospinning device was varied by a heating system. The resulting nonwoven mats were characterized by using scanning electron microscopy (SEM), field emission SEM (FESEM), and atomic force microscopy (AFM). We observed that the surface morphology, porous structure, and the properties such as pore size, depth, shape, and distribution of the nonwoven mats were greatly influenced by the collector temperature.

Keywords: electrospinning, morphology, porous structure, poly(L-lactide), polystyrene, poly(vinyl acetate).

Introduction

Advancements in the scientific and technical knowledge about electrospinning have a significant effect on the industry as well as society, and opened up a new field. Electrospinning processes have attracted a great deal of attention in regard to obtain smaller fibers. Fiber diameters produced by conventional methods range from 1 to 500 μm,[1] whereas electrospun fibers have diameters in the submicron to nanometer range.[2] During electrospinning, a strong electric field is applied between a polymer solution contained in a syringe with a capillary tip and grounded metallic collector using a high voltage supply. When the applied voltage reaches a critical value, charged jet was ejected as a droplet. The charged jets experience bending instabilities while traveling to the collector and the droplets were split into bundles of small fibers. This phenomenon relates to the rapid solvent evaporation and a reduction in the diameter of the jet.[3-5]As soon as the jet reaches the collector, the solidified fibers are accumulated onto the grounded collector.

It is well known that the morphology of electrospun nonwoven mats can be influenced by many factors, such as polymer, solvent boiling point, surface tension, solution viscosity, solution conductivity, solution concentration, glass transition temperature (T_g) of the polymer, applied voltage, and tip to collector distance (TCD).[6,7] Certain electrospun polymeric nanofibers have unique morphology with porous nature.[8-10] Earlier reports showed that when a solution of poly(L-lactide) (PLLA), polycarbonate (PC), polyvinylcarbazole, poly(methyl methacrylate) (PMMA), poly(ethylene oxide) (PEO), and polystyrene (PS) in highly volatile solvents was electrospun, many pores appear on the surface of electrospun fibers.[7-10] There are two possible mechanisms that have been related to the formation of pores on the surface of electrospun fibers. One is the breath figure mechanism and the other is thermally induced phase separation (TIPS). Both the mechanisms are strongly related to the temperature.[9,10] When the jet was ejected out from the tip of the syringe, it is cooled, also water in the air is condensed on the surface of electrospun fiber and subsequently the solvent and nonsolvent are evaporated.[2,6-10] Hence, evaporation of solvent plays an important role in the formation of pores on the surface of the electrospun fiber. Thus, we believed that the temperature of the collector is an important factor to manipulate the surface morphology of electrospun fiber.

The presence of porous structure in the electrospun fiber, having an ultra large surface-volume ratio, is a very useful property for applications in tissue engineering, wound dress-

*Corresponding Author. E-mail: khy@chonbuk.ac.kr

ing, and artificial blood vessel, etc.[11-21] The porous surface of electrospun scaffolds or mats might be helpful for an increase in cell attachment and tissue compatibility.[11-21] For example, porous structure can affect the wetting behavior, as well as specific adsorption processes. Sometimes, samples prepared from the same material, show different tissue biocompatibility, depending on their morphology.[19] Also, abnormal encapsulation of implanted materials by the surrounding tissue, chronic inflammation around implanted materials, and induction of carcinoma by implanted materials are related to the surface topography.[22-26]

Based on the above facts, we proposed to investigate the effect of collector temperature on the surface characteristics of electrospun PLLA, PS, and poly(vinyl acetate) (PVAc) nonwoven mats. We also made an effort to control the size and distribution of pores in electrospun nonwoven mats as a function of a collector temperature.

Experimental

Materials. PLLA (M_w=650,000) and PVAc (M_w=140,000) were purchased from Boehringer Ingelheim Co. and McGean Co., respectively. PLLA and PVAc were dissolved separately in methylene chloride (MC) upto a final concentration of 3.5 and 10 wt%, respectively. PS (M_n=140,000) was purchased from Aldrich Co. and dissolved in tetrahydrofuran (THF) to get 25 wt% solution for electrospinning. All the polymers were used as received without further purification. The solvents were purified by distillation before use.

Electrospinning. High voltage power supply (CPS-60 k02v1, Chungpa EMT, Co., Korea) was used to generate voltage in a range of 0-50 kV. Polymer solution was filled into the 5 mL plastic syringe with 1 mm diameter tip, which was placed at angle of 10° to the horizontal in order to get uniform flow of the solution. The applied voltage and tip-to-collector distance were in the range of 12-15 kV and 10-15 cm, respectively. A copper wire attached to a positive electrode was inserted into the polymer solution. The negative electrode was attached to the ground metal collector, which in turn was connected to a heater with variable temperature control. A uniform temperature over the whole collector area was checked at regular intervals. In this work, a vacuum desiccator was introduced to maintain temperature and humidity at a constant value. The temperature and humidity during electrospinning were fixed at 21 °C and 60%, respectively. The schematic diagram of the instrumental setup used in this experiment is shown in Figure 1. The nonwoven mats deposited on the collector were removed and characterized by various methods.

Morphology. The surface morphology of electrospun nonwoven mats was investigated using SEM (GSM-5900, JEOL. Co., Japan) and FESEM (S-4700, HITACHI Co., Japan) instruments. Prior to the observation, samples were coated with gold. The surface topology was analyzed using atomic force microscopy (AFM), which has a Scanning Probe Microscope (Nanoscope IIIa, Multimode™ SPM, version 4.31ce from Digital Instruments Co., USA). A contact with lateral force and tapping with phase imaging were introduced to measure the topology under ambient conditions. Several samples were scanned, and each sample was imaged at different areas to check the lateral uniformity. All images were provided in the text without any image processing, except horizontal leveling and contrast enhancement. AFM analysis allowed for the calculation of surface area of the electrospun porous fiber.

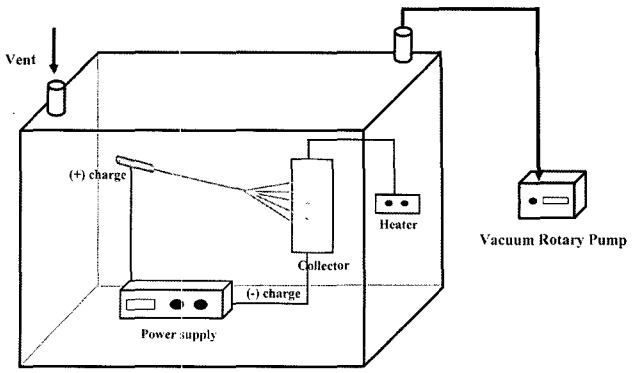

Figure 1. Schematic diagram of the electrospinning device under vacuum condition.

Results and Discussion

This experiment was carried out using semi-crystalline PLLA, amorphous PS, and PVAc. In particular, PLLA has received much attention and achieved a large commercial success, due to its biomedical applicability and biodegradability. PLLA solution in MC was electrospun (concentration 3.5 wt%, applied voltage 15 kV, and TCD 15 cm) at five different collector temperatures (21 (RT), 40, 50, 60, and 70 °C) to examine the influence of collector temperature on the topology of the fibers produced. Figure 2 shows the SEM images of electrospun PLLA fibers as a function of collector temperature. At room temperature (21 °C) (Figure 2(a)), a number of small pores were seen on the surface of the electrospun fiber. The pore size was increased by heating the collector at 40 °C (Figure 2(b)). This behavior can be attributed to the boiling point of the solvent used for electrospinning solution (MC).[10] During the electrospinning process, the solvent usually evaporates on its travel from the tip of the syringe to collector.[2] But the residual solvents entrapped inside the fiber were evaporated by heating the collector at the temperature equivalent or nearly equivalent to the solvent boiling point. Hence the pores with larger diameter were formed due to the accelerated evaporation of solvent. A marked difference in the morphology and pore shape and size of the electrospun PLLA fibers are observed

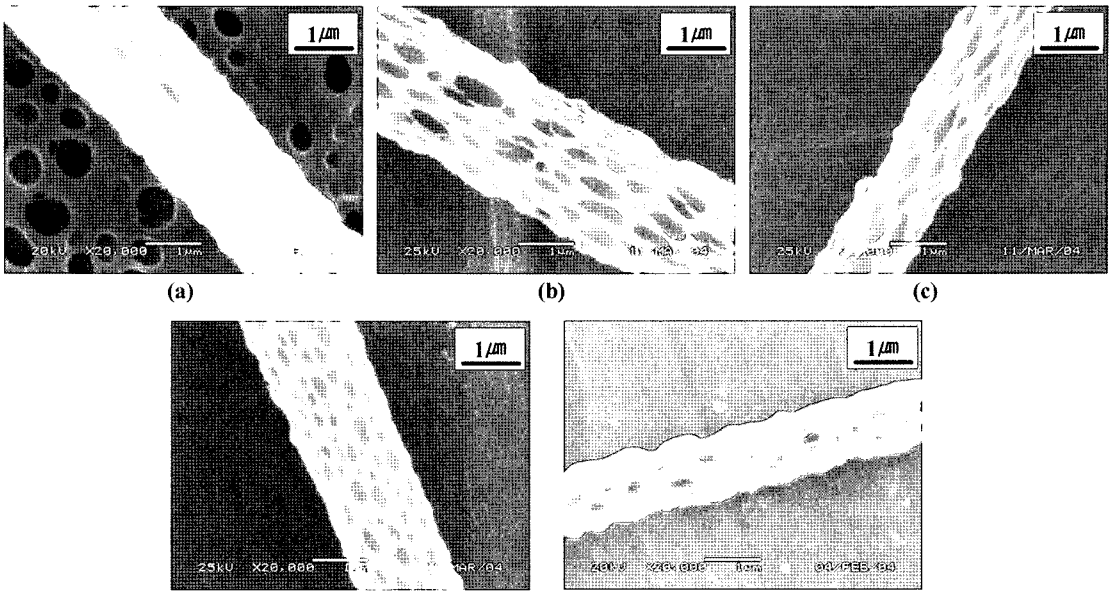

Figure 2. SEM images of electrospun PLLA fibers as a function of collector temperature; (a) room temperature (21 °C), (b) 40, (c) 50, (d) 60 , and (e) 70 °C.

at a collector temperature of 50 °C due to rapid evaporation of MC at a temperature higher than its boiling point and viscoelastic nature of the polymer at this temperature (Figure 2(c)). Further, when the collector was heated to 60 °C, the pore size was reduced (Figure 2(d)). It is clear that at this temperature, the solvent vapors formed inside the viscose melt were released at once, due to acceleration in the volatility of MC resulting in the formation of many small pores. Further, as the collector temperature approaches T_g of PLLA, the pore structure on the surface of fiber collapsed, owing to the insufficient solidification and comparatively high mobility of PLLA at this temperature. Figure 2(e) shows that the pores obtained at a collector temperature of 70 °C (above the T_g of PLLA). Similar results were also obtained in the case of electrospun nanofibers of amorphous PS and PVAc dissolved in THF and MC, respectively. This phenomenon suggest that the pore shape and size are influenced strongly by both the boiling point of the solvent and T_g of polymer in addition to the temperature of the collector.

To investigate the effect of the collector temperature on the pore properties like pore depth, pore diameter, and surface area of electrospun PLLA, AFM images were recorded and shown in Figure 3. The height profiles correspond to the marked directions from top to bottom and the reference positions are marked 0. The details of pore depth and surface area of the electrospun PLLA fiber at different collector temperatures are presented in Table I. As we observed in the SEM images (Figure 2(c)), a high magnitude of pore depth and surface area were found in the AFM images at a collector temperature of 50 °C (Figure 3(c)), at temperatures above and below 50 °C.

Figure 4 shows the ratio of the pore width to pore length of PLLA fibers at each collector temperature. Here, the pore width means the distance perpendicular to the axis fiber direction, whereas pore length is the distance parallel to the fiber. This result shows that the ratio of pore width to pore length is increased as the temperature is increased, which means that the shape of the pore is closer to a perfect circle. The shape of pore, in particular, becomes more linear between the boiling point of MC (40 °C) and T_g of PLLA (60 °C). This data revealed that the shape of pores on fiber surface is related to both the boiling point of solvent and T_g of polymer.

In line with the above observations, we also carried out the electrospinning of amorphous PS under suitable conditions (concentration 25 wt%, applied voltage 15 kV, and TCD 15 cm). Figure 5 shows FESEM images of electrospun PS nonwoven mats as a function of the collector temperature. A 25 wt% of PS solution in THF was electrospun at room temperature (21 °C), 40, 60, 80, and 100 °C, respectively. Figures 5(a) and (b) show similar morphology on the surface of electrospun fibers. However, a lot of pores were formed, when the collector temperature was around the boiling point of THF (66 °C), as shown in Figure 5(c). Figure 5(e) reveals that the pores obtained above the T_g of PS (100 °C) were not in order and collapsed in shape.

In addition, to investigate the effect of the collector temperature on the topology of pores, AFM images were recorded and shown in Figure 6. The measurements of pore depth and surface area of the electrospun PS fibers by varying the collector temperature are given in Table II. From the AFM images and data presented in the Table II, it was found

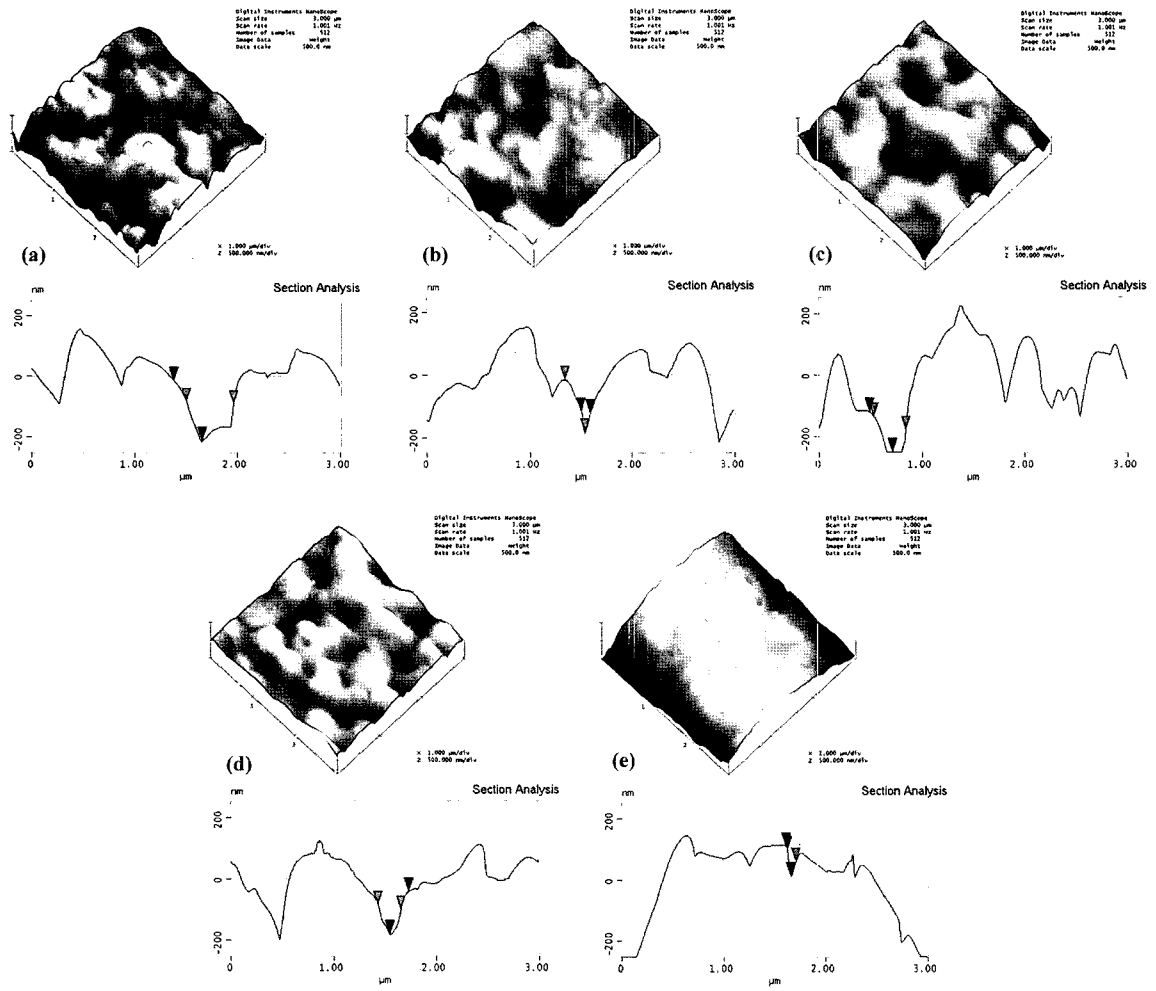

Figure 3. AFM images of electrospun PLLA fibers as a function of collector temperature; (a) room temperature (21 °C), (b) 40, (c) 50, (d) 60, and (e) 70 °C.

Table I. Pore Depth and Surface Area of Electrospun PLLA Nonwoven Mats as a Function of Collector Temperature

Collector Temperature (°C)	Range of Pore Depth (nm)	Average of Pore Depth (nm)	Surface Area (μm^2)[a]
RT	80-180	160	13.67
40	90-290	210	15.9
50	110-460	270	16.12
60	100-270	180	14.4
70	30-150	110	11.37

[a]The projected surface for all the 3×3 μm^2 images presented in this table is 9 μm^2.

that pore depth and surface area increased with collector temperature until 60 °C (Figure 6(c)), whereas it decreased above and below 60 °C.

Figure 7 displays the FESEM images of electrospun PVAc

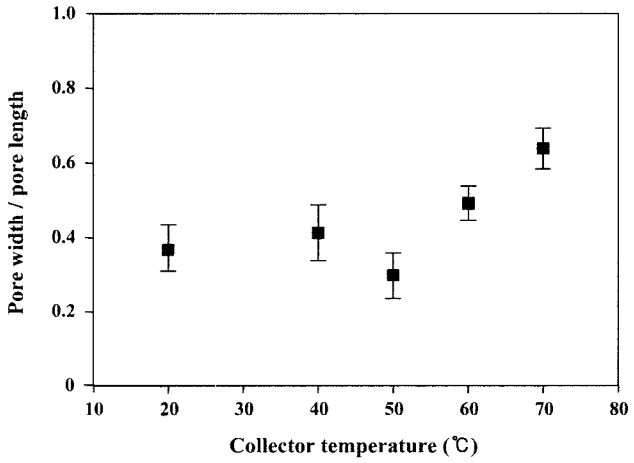

Figure 4. Ratio of pore width and length of PLLA fibers as a function of collector temperature. Here, the pore width means the distance perpendicular to the axial fiber direction, whereas pore length is the distance parallel to the fiber. Data are means ± SD, n = 5.

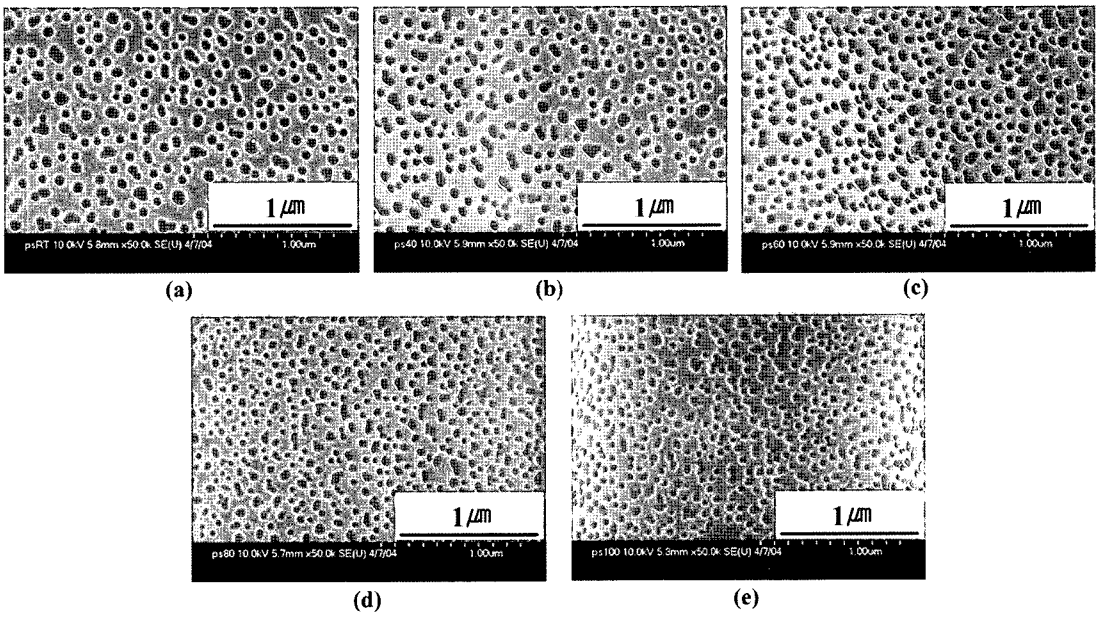

Figure 5. FESEM images of electrospun PS fibers as a function of collector temperature; (a) room temperature (21 °C), (b) 40, (c) 60, (d) 80, and (e) 100 °C.

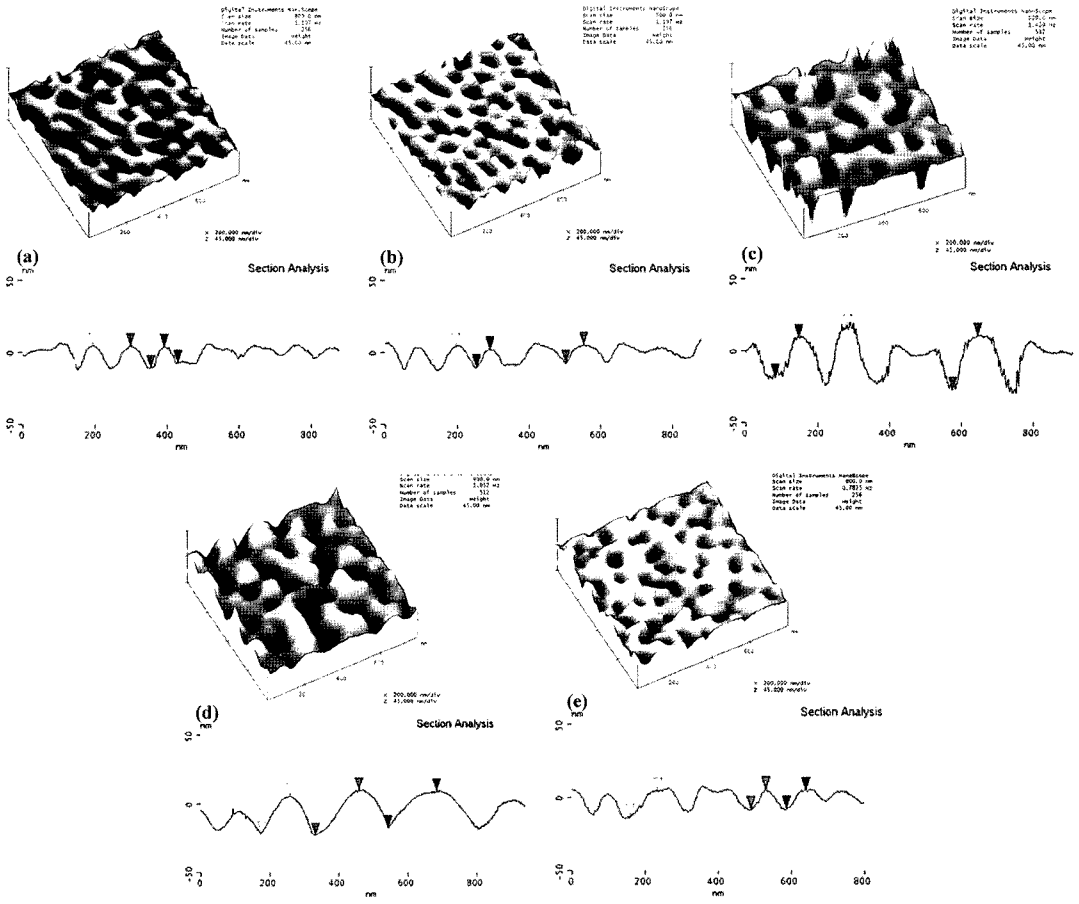

Figure 6. AFM images of electrospun PS fibers as a function of collector temperature; (a) room temperature (21 °C), (b) 40, (c) 60, (d) 80, and (e) 100 °C.

Table II. Pore Depth and Surface Area of Electrospun PS Nonwoven Mats as a Function of Collector Temperature

Collector Temperature (°C)	Range of Pore Depth (nm)	Average of Pore Depth (nm)	Surface Area (μm^2)[a]
RT	5-12	9	5.24
40	7-13	10	6.09
60	26-45	37	7.35
80	21-34	31	7.14
100	8.12	12	5.43

[a]The projected surface for all the 2×2 μm^2 images presented in this table is 4 μm^2.

nonwoven mats as a function of the collector temperature. A 10 wt% PVAc solution in THF was electrospun under appropriate conditions (concentration 10 wt%, applied voltage 12 kV, and TCD 15) at various collector temperatures such as room temperature (21 °C), 30, 40 , 50, and 100 °C, respectively. The surface morphology of the PVAc nonwoven fibers produced at 21 °C (room temperature) is shown in Figure 7(a). This figure showed the presence of ordered pore arrangement with uniform diameter and distribution on the fiber surface. Figure 7(b) demonstrated that the pore structure on the surface of electrospun PVAc fibers were poorly defined at 30 °C, due to the low T_g (28 °C) of PVAc.[27] The morphology observed in the Figures 7(c), (d), and (e) corresponding to the collector temperatures higher than the T_g of PVAc was found to be different from that below T_g of PVAc.

In this study, PLLA, PS, and PVAc dissolved in solvents that have low boiling point were successfully electrospun to manipulate the porous structure on the surface of fiber by changing the temperature of collector. As the temperature of collector reaches the boiling point of solvent, the evaporation of solvent was accelerated during the electrospinning process. Such rapid evaporation of solvent results in the formation of pores. However, as the temperature of the collector approaches T_g of polymer used, the porous structure on the surface of fiber collapsed, owing to the insufficient solidification and comparatively high mobility of polymer used around T_g.

Generally, there are two mechanisms that have been used to explain the formation of pores on the surface of electrospun nonwoven mats.[9,10] Following the breath figure mechanism, the solvent within the polymer jet will evaporate as the jet travels to the collector. The jet meets moisture on the air and the fiber was subsequently mounted on the collector, condensed along with moisture as soon as it hit the surface of collector. Both solvent and condensed water evaporate from the surface of electrospun fiber, and they remain in traces in the surface or interior of fibers, which finally escaped out to form pores. From this point of view, the evaporating rate of both condensed water and residual solvent inside the fiber depend on the temperature of collector. The topology, such as size and distribution of a pore can be controlled by changing the temperature of collector.

Another mechanism for the formation of pores on the surface of electrospun fiber is phase separation. There are various phase separation methods to prepare porous membranes such as TIPS, immersion precipitation, air-casting of the

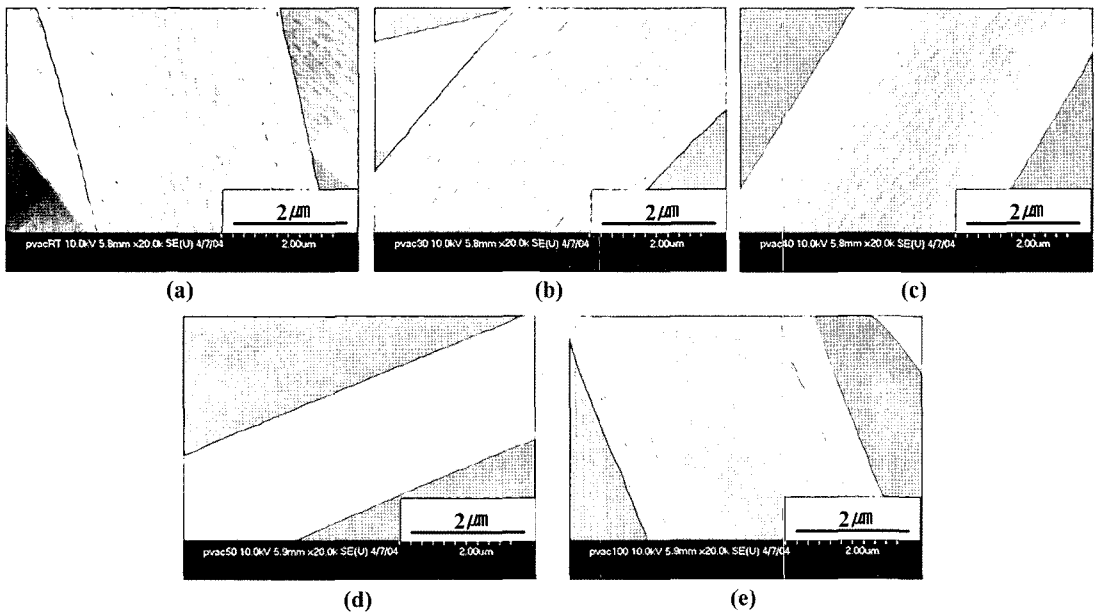

Figure 7. FESEM images of electrospun PVAc fibers as a function of collector temperature; (a) room temperature (21 °C), (b) 30, (c) 40, (d) 50, and (e) 100 °C.

polymer solution, and vapor-induced phase separation.[28] All these phenomena are well-known and discussed in the literature.[9,10] TIPS involves rapid evaporation of solvent and vapor induced phase separation involves the penetration of nonsolvent vapor.[9,10] When the jet is cooled, water is condensed and both the solvent and nonsolvent (water) are evaporated. At this time, the temperature of the collector plays a major role in accelerating the evaporation of the solvent and nonsolvent. Thus, it is certain that the change in surface morphology of electrospun nonwoven mats is correlated to the collector temperature. Bognitzki *et al.* introduced phase separation to explain the presence of pores in the electrospun PLLA, PC, and polyvinylcarbazole mats dissolved in MC.[8] They illustrated that solvent evaporation in the domain with abundant solvent involves more rapid phase separation, which results in the porous structure on the surface of the electrospun fiber. Though we cannot differentiate whether breath figure or phase separation is responsible for the formation of pores, it is certain that temperature is an important factor in determining the porous structure.

Conclusions

A systematic study on the surface topography of the nonwoven mats such as pore size and distribution of pore prepared by electrospinning was undertaken as a function of the collector temperature. From the obtained results, we conclude that the morphology of electrospun PLLA, PS, and PVAc nonwoven mats using a volatile solvent was strongly related to both the boiling point of solvent and T_g of polymer. Therefore, the topology such as pore size, pore depth, and distribution of pores can be controlled by changing the temperature of collector. In order to explain the changes of pores on electrospun nonwoven mats, as a function of the temperature of collector, both breathe figure and phase separation mechanism were discussed. Hence, the introduction of a temperature controllable collector in the electrospinning device is a simple and novel method to fabricate the electrospun nonwoven mats with porous surface that will make the fibers to be customized for specific uses in the high efficiency filtration and tissue engineering field.

Acknowledgements. This work was supported by the Regional Research Center Program of the Korean Ministry of Education & Human Resources Development, through the Center for Health Care Technology Development, Chonbuk National University, Chonju 561-756, Republic of Korea.

References

(1) A. Ziabicki, Fundamentals of Fiber Formation: the Science of Fiber Spinning and Drawing, Wiley, New York, 1976.
(2) Y. J. Ryu, H. Y. Kim, K. H. Lee, H. C. Park, and D. R. Lee *Eur. Polym. J.*, **39**, 1883 (2003).
(3) M. M. Hohman, M. Shin, G. C. Rutledge, and M. P. Brenner *Phys. Fluids*, **13**, 2221 (2001).
(4) P. K. Baumgarten, *J. Colloid Interf. Sci.*, **36**, 71 (1971).
(5) D. H. Reneker, A. L. Yarin, H. Fong, and S. Koombhongse *J. Appl. Phys.*, **87**, 4531 (2000).
(6) K. H. Lee, H. Y. Kim, Y. M. La, D. R. Lee, and N. H. Sung, *J. Polym. Sci.; Part B: Polym. Phys.*, **40**, 2259 (2002).
(7) M. Bognitzki, H. Hou, M. Ishaque, T. Frese, M. Hellwig, C. Schwarte, A. Schaper, J. H. Wendorff and A. Greiner, *Adv. Mater.*, **12**, 637 (2000).
(8) M. Bognitzki, W. Czado, T. Frese, A. Schaper, M. Hellwig, M. Steinhart, A. Greiner, and J. H. Wendorff, *Adv. Mater.*, **13**, 70 (2001).
(9) C. L. Casper, J. S. Stephens, N. G. Tassi, D. B. Chase, and J. F. Rabolt, *Macromolecules*, **37**, 573 (2004).
(10) S. Megelski, J. S. Stephens, D. B. Chase, and J. F. Rabolt, *Macromolecules*, **35**, 8456 (2002).
(11) D. H. Reneker and I. Chun, *Nanotechnology*, **36**, 169 (1997).
(12) C. J. Buchko, L. C. Chen, Y. Shen, and D. C. Martin, *Polymer*, **40**, 7397 (1999).
(13) L. Huang, R. A. McMillan, R. P. Apkarian, B. Pourdeyhimi, V. P. Conticello, and E. L. Chaikof, *Macromolecules*, **33**, 2989 (2000).
(14) L. Huang, K. Nagapudi, R. P. Apkarian, and E. L. Chaikof, *J. Biomater. Sci. Polym. Ed.*, **12**, 979 (2001).
(15) J. D. Stitzel, G. L. Bowlin, K. Mansfield, G. E. Wnek, and D. G. Simpson, *Int. SAMPE Tech. Conf.*, **32**, 205 (2000).
(16) E. D. Boland, G. E. Wnek, D. G. Simpson, K. J. Pawlowski, and G. L. Bowlin, *J. Macromol. Sci. Pure Appl. Chem.*, **A38**, 1231 (2001).
(17) X. Zong, K. Kim, D. Fang, S. Ran, B. S. Hsiao, and B. Chu, *Polymer*, **43**, 4403 (2002).
(18) K. Nagapudi, W. T. Brinkman, J. E. Leisen, L. Huang, R. A. McMillan, R. P. Apkarian, V. P. Conticello, and E. L. Chaikof, *Macromolecules*, **35**, 1730 (2002).
(19) J. A. Matthews, G. E. Wnek, D. G. Simpson, and G. L. Bowlin, *Biomacromolecules*, **3**, 232 (2002).
(20) W. J. Li, C. T. Laurencin, E. J. Caterson, R. S. Tuan, and F. K. Ko, *J. Biomed. Mater. Res.*, **60**, 613 (2002).
(21) E. R. Kenawy, J. M. Layman, J. R. Watkins, G. L. Bowlin, J. A. Matthews, S. G. Simpson, and G. E. Wnek, *Biomaterials*, **24**, 907 (2003).
(22) B. D. Ratner, *Trends Polym. Sci.*, **2**, 402 (1994).
(23) J. Schmidt and A. F. von Recum, *Biomaterials*, **13**, 1059 (1992).
(24) A. Curtis and C. Wilkinson, *Biomaterials*, **18**, 1 (1997).
(25) E. Richter, G. Fuhr, T. MuÈller, S. Shirley, S. Rogaschewski, K. Reimer, and C. Dell, *J. Mater. Sci. Mater. Med.*, **7**, 85 (1996).
(26) W. Liu, Z. Wu, and D. H. Reneker, *Polym. Prepr.*, **41**, 1193 (2000).
(27) A. C. Backman and K. A. H. Lindberg, *J. Appl. Polym. Sci.*, **91**, 3009 (2004).
(28) H. Matsuyama, M. Teramoto, R. Nakatani, and T. Maki, *J. Appl. Polym. Sci.*, **74**, 171 (1999).